1-1-2015

Rhabdovirus-based vaccine platforms against henipaviruses.

Drishya Kurup
Department of Microbiology and Immunology, Sidney Kimmel Medical College, Thomas Jefferson University, Drishya.Kurup@jefferson.edu

Christoph Wirblich
Department of Microbiology and Immunology, Sidney Kimmel Medical College, Thomas Jefferson University, Christoph.Wirblich@jefferson.edu

Heinz Feldmann
Laboratory of Virology, Division of Intramural Research, National Institute of Allergy and Infectious Diseases, National Institutes of Health, Hamilton, MT

Andrea Marzi
Laboratory of Virology, Division of Intramural Research, National Institute of Allergy and Infectious Diseases, National Institutes of Health, Hamilton, MT

Matthias J. Schnell
Department of Microbiology and Immunology, Sidney Kimmel Medical College, Thomas Jefferson University; Jefferson Vaccine Center, Sidney Kimmel Medical College, Thomas Jefferson University, Matthias.Schnell@jefferson.edu

JVI Journals.ASM.org

Rhabdovirus-Based Vaccine Platforms against Henipaviruses

Drishya Kurup,[a] Christoph Wirblich,[a] Heinz Feldmann,[b] Andrea Marzi,[b] Matthias J. Schnell[a,c]

Department of Microbiology and Immunology[a] and Jefferson Vaccine Center,[c] Sidney Kimmel Medical College, Thomas Jefferson University, Philadelphia, Pennsylvania, USA; Laboratory of Virology, Division of Intramural Research, National Institute of Allergy and Infectious Diseases, National Institutes of Health, Hamilton, Montana, USA[b]

ABSTRACT

The emerging zoonotic pathogens Hendra virus (HeV) and Nipah virus (NiV) are in the genus *Henipavirus* in the family *Paramyxoviridae*. HeV and NiV infections can be highly fatal to humans and livestock. The goal of this study was to develop candidate vaccines against henipaviruses utilizing two well-established rhabdoviral vaccine vector platforms, recombinant rabies virus (RABV) and recombinant vesicular stomatitis virus (VSV), expressing either the codon-optimized or the wild-type (wt) HeV glycoprotein (G) gene. The RABV vector expressing the codon-optimized HeV G showed a 2- to 3-fold increase in incorporation compared to the RABV vector expressing wt HeV G. There was no significant difference in HeV G incorporation in the VSV vectors expressing either wt or codon-optimized HeV G. Mice inoculated intranasally with any of these live recombinant viruses showed no signs of disease, including weight loss, indicating that HeV G expression and incorporation did not increase the neurotropism of the vaccine vectors. To test the immunogenicity of the vaccine candidates, we immunized mice intramuscularly with either one dose of the live vaccines or 3 doses of 10 μg chemically inactivated viral particles. Increased codon-optimized HeV G incorporation into RABV virions resulted in higher antibody titers against HeV G compared to inactivated RABV virions expressing wt HeV G. The live VSV vectors induced more HeV G-specific antibodies as well as higher levels of HeV neutralizing antibodies than the RABV vectors. In the case of killed particles, HeV neutralizing serum titers were very similar between the two platforms. These results indicated that killed RABV with codon-optimized HeV G should be the vector of choice as a dual vaccine in areas where rabies is endemic.

IMPORTANCE

Scientists have been tracking two new viruses carried by the Pteropid fruit bats: Hendra virus (HeV) and Nipah virus (NiV). Both viruses can be fatal to humans and also pose a serious risk to domestic animals. A recent escalation in the frequency of outbreaks has increased the need for a vaccine that prevents HeV and NiV infections. In this study, we performed an extensive comparison of live and killed particles of two recombinant rhabdoviral vectors, rabies virus and vesicular stomatitis virus (VSV), expressing wild-type or codon-optimized HeV glycoprotein, with the goal of developing a candidate vaccine against HeV. Based on our data from the presented mouse immunogenicity studies, we conclude that a killed RABV vaccine would be highly effective against HeV infections and would make an excellent vaccine candidate in areas where both RABV and henipaviruses pose a threat to human health.

Hendra virus (HeV) and Nipah virus (NiV) are emerging zoonotic viruses that belong to the *Henipavirus* genus within the *Paramyxoviridae* family. Both are highly pathogenic in humans.

Henipaviruses are naturally harbored by Pteropid fruit bats (commonly referred to as flying foxes) that undergo asymptomatic infections (1). Henipavirus-associated disease was initially detected in horses and pigs, which likely were in contact with infective bat urine or droppings or contaminated fruit (2). However, both viruses can infect a wide range of animal species (wild or domestic), including humans. HeV and NiV have host-specific respiratory or neurological tropism, and infections are associated with high morbidity and case fatality rates of up to 75% (1, 3). Henipaviruses are classified as biosafety level 4 (BSL4) pathogens and considered to be bioterrorism and agroterrorism threats, which increases the need for development and production of safe and effective vaccines for livestock and humans (2, 4).

HeV emerged in 1994 in two separate outbreaks of severe respiratory disease in horses with subsequent transmission to humans, who were in close contact with the infected horses (5). Although initially called "equine morbillivirus," because both of the initial outbreaks involved horses, it was renamed "HeV" after the first outbreak in the Brisbane suburb of Hendra, Queensland, Australia. Investigations revealed that *Pteropus* species bats are the primary reservoir of HeV (6).

NiV emerged in 1998 in a major outbreak of acute febrile encephalitis in humans in Malaysia that resulted in 265 human cases and 105 fatalities. The virus was named after the first isolated case in a patient from the Sungai Nipah village. Investigations revealed that the outbreak originated from infected pigs, in which the virus caused a mild disease, but was then transmitted to humans through close contact with the pigs (7, 8). In humans, both HeV and NiV infections cause respiratory disease and/or severe neuro-

Received 8 August 2014 Accepted 2 October 2014

Accepted manuscript posted online 15 October 2014

Citation Kurup D, Wirblich C, Feldmann H, Marzi A, Matthias JS. 2015. Rhabdovirus-based vaccine platforms against henipaviruses. J Virol 89:144–154. doi:10.1128/JVI.02308-14.

Editor: D. S. Lyles

Address correspondence to Matthias J. Schnell, Matthias.Schnell@jefferson.edu.

doi:10.1128/JVI.02308-14

logical disease that may eventually progress to coma and finally death (1). HeV infection in horses predominantly causes death due to severe respiratory disease, and the horses may show some neurological symptoms (5).

Virus attachment, membrane fusion, and particle entry for HeV and NiV requires two distinct, membrane-anchored glycoproteins: (i) a fusion (F) glycoprotein (type I membrane protein) mediating the fusion of the viral and host cell membranes and (ii) an attachment (G) glycoprotein (type II membrane protein) required for receptor binding and virion attachment to the host cell. HeV G and HeV F share a high degree (83% to 89%) of similarity to NiV G and NiV F (9).

The ability of henipaviruses to infect a wide range of mammalian species appears to be linked to their cellular receptors, ephrins B2 and B3 (10). Ephrin receptors are highly conserved across species and to be involved in mediating short-range cell-to-cell communication (11). Ephrin B2 is expressed in endothelial cells, smooth muscle cells, bronchial epithelial cells, and cardiomyocytes, whereas ephrin B3 is mostly restricted to the central nervous system (12, 13). Notably, ephrins B2 and B3 have been identified as functional receptors for HeV and NiV via their G glycoproteins (9, 10), but NiV appears to have a higher affinity for ephrin B3 than HeV, which could explain the stronger neurotropism of NiV (14).

Currently, researchers are exploring three different approaches for the prevention and/or treatment of henipavirus infections. The first approach utilizes human monoclonal antibodies (MAb) that were selected from a human Fab phage display library for their high binding to soluble HeV glycoprotein (sG). In particular, the m102 antibody possessed potent virus-neutralizing activity (15), which was further improved by *in vitro* maturation. This improved MAb (m102.4) has been shown to protect ferrets from lethal NiV challenge and African green monkeys (AGM) from lethal HeV and lethal NiV challenge (16–19).

The second approach utilizes viral vaccines. Protection against Nipah virus challenge was reported for recombinant vesicular stomatitis virus (VSV) and adeno-associated virus 8 (AAV8) viral vaccines in the Syrian Hamster and ferret models (20–22). The AAV8-NiV G vaccine also conferred partial cross-protection against HeV challenge (23).

The third approach utilizes a recombinant subunit vaccine sG_{HeV} (containing an engineered secreted version of the full ectodomain of HeV G) that protects against both HeV and NiV challenge in the AGM model, which recapitulates the severe clinical symptoms and pathology associated with henipavirus infection in humans (24, 25) Furthermore, the subunit vaccine Equivac HeV demonstrated complete protection in horses and is now used by the equine industry in Australia (26).

In our study, we aimed to develop a rhabdovirus-based vaccine against HeV for humans and animals. Both, rabies virus (RABV) and vesicular stomatitis virus (VSV) are members of the *Rhabdoviridae* family and are relatively simple, enveloped, negative-stranded RNA viruses that encode five proteins (N, P, M, G, and L). Vaccines based on both viruses have been shown to induce potent humoral responses against other viral pathogens, but the vectors have never been compared in parallel for the same pathogen. Our recombinant RABV vaccine vector is derived from the live-attenuated RABV strain SAD B19 RABV, which is licensed and used for wildlife vaccination in Europe and is nonpathogenic in a wide range of animal species when administered orally or intramuscularly (27–30). This strain was further attenuated by switching an amino acid in the RABV glycoprotein (G), which greatly reduces the neurotropism of the RABV strain (28, 31). The recombinant VSV platform utilized here is an attenuated VSV Indiana strain that was previously shown to be safe in small animal models (32, 33). Both recombinant RABV- and VSV-based vaccine vectors have been shown to be safe and immunogenic in nonhuman primates (33, 34).

MATERIALS AND METHODS

Antibodies. The human monoclonal antibody 4C12 against RABV glycoprotein was provided by Scott Dessain (Lankenau Institute for Medical Research, Wynnewood, PA), the mouse monoclonal antibody 41C3 against HeV glycoprotein was a generous gift from Christopher Broder (Uniformed Services University, Bethesda, MD), and the hybridomas producing monoclonal antibodies I1 and I14 against VSV glycoprotein were provided by John Rose (Yale University, New Haven, CT).

cDNA construction of vaccine vectors. We inserted codon-optimized Hendra virus glycoprotein gene G (for vaccine "coHeVG" constructs [gene synthesized by Genscript USA, Inc.]) or wild-type (wt) Hendra glycoprotein gene G (for vaccine "HeVG" constructs) into the BsiWI and NheI restriction sites of the BNSP333 RABV vector (30). The resulting plasmids were designated RABV-coHeVG and RABV-HeVG, respectively. The VSV-based vaccines were made by PCR amplification of the coding region of HeVG with primers RP1163 (ATTACTCGAGGCCACC ATGATGGCTGATTCCAAATTGGTAG) and RP1088 (GAGAGCTAGC TTATCAACTCTCTGAACATTGGGCAGGT) or the coding region of coHeVG with primers RP1170 (ACTGTACTCGAGGCCGCCACCATG ATGGCCGACTCTAAACTGGTC) and RP1171 (ACTGTAGCTAGCT CAGGACTCGCTGCACTGAGCTGGGAT). The resulting PCR products were inserted into the XhoI and NheI restriction sites (between the G and L genes) of the VSV vector cVSV-XN (35). The resulting plasmids were designated VSV-HeVG and VSV-coHeVG, respectively. The correct sequences of all four plasmids were confirmed by sequencing.

Recovery of recombinant vectors. Recombinant RABV and VSV were recovered as described previously (36, 37). Briefly, X-tremeGENE 9 transfection reagent (Roche Diagnostics) in Opti-MEM was used to cotransfect the respective full-length viral cDNA clones along with the plasmids encoding RABV N, P, G, and L or VSV N, P, and L proteins and the T7 RNA polymerase into BSR cells in 6-well plates (RABV) or 293T cells in T25 flasks (VSV). We harvested the supernatants of transfected cells after 7 days for transfection with RABV and after 3 days for VSV recoveries. We then analyzed for the presence of infectious virus by immunostaining for RABV or for virus-induced cytopathic effect (CPE) in the case of VSV.

Sucrose purification and inactivation of the virus particles. Larger amounts of RABV-HeVG or RABV-coHeVG were concentrated in a stirred 300-ml ultrafiltration cell (Millipore) and then spun through a 20% sucrose cushion in an SW32 Ti rotor (Beckman, Inc.) at 25,000 rpm for 1.5 h. Recombinant VSVs were purified similarly but without prior concentration in ultrafiltration cells. Virion pellets were resuspended in phosphate-buffered saline (PBS), and protein concentrations were determined using a bicinchoninic acid (BCA) assay kit (Pierce). The virus particles were inactivated with 50 μl per mg of particles of a 1:100 dilution of β-propiolactone (BPL) in cold water. The absence of infectious particles was verified by inoculating BSR cells with 10 μg of BPL-inactivated viruses. After 4 days of incubation at 34°C, the cells were subcultured and 500 μl of supernatant was passaged on fresh BSR cells. Cultures were examined 4 days later for absence of cytopathogenicity for VSV and lack of staining with a fluorescein isothiocyanate (FITC)-conjugated anti-RABV N MAb for RABV.

Virus characterization. The virus particles were denatured with urea buffer (125 mM Tris-HCl [pH 6.8], 8 M urea, 4% sodium dodecyl sulfate, 5% β-mercaptoethanol, 0.02% bromophenol blue) at 95°C for 5 min. Three micrograms of protein was resolved on a 10% SDS–polyacrylamide gel and thereafter stained overnight with SYPRO Ruby for total protein

analysis or transferred onto a nitrocellulose membrane in Towbin buffer (192 mM glycine, 25 mm Tris, 20% methanol) for Western blot analysis. The nitrocellulose membrane was then blocked in TBST (100 mM Tris-HCl [pH 7.9], 150 mM NaCl, 0.05% Tween 20) containing 5% dried milk at room temperature for 1 h. After blocking, the membrane was incubated overnight with antisera obtained from a convalescent HeV-infected African green monkey at a dilution of 1:1,000 in 5% bovine serum albumin (BSA). After washing, the blot was incubated for 1 h with horseradish peroxidase (HRP)-conjugated anti-human IgG diluted 1:50,000 in blocking buffer. Bands were developed with SuperSignal West Dura Chemiluminescent substrate (Pierce). The incorporation of HeV G was compared between the different cell lines, wt and coHevG-expressing viruses, and also between the two rhabdovirus vectors utilizing AlphaView software (ProteinSimple) for quantification of SYPRO Ruby-stained SDS-PAGE gels. To account for differences in particle load, the amount of HeV G was normalized to the amount of RABV or VSV N, which is equal for particles with the same genome length.

FACS analysis. A total of 8×10^5 Vero cells were seeded in 6-well plates. For the VSV fluorescence-activated cell sorter (FACS) analysis, cells were infected with VSV-HeVG, VSV-coHeVG, or VSV expressing Zaire Ebola virus (ZEBOV) glycoprotein (VSV-ZGP) at a multiplicity of infection (MOI) of 5 or left uninfected (control) for 6.5 h. For the RABV FACS analysis, cells were infected with RABV-HeVG, RABV-coHeVG, or RABV at an MOI of 10 or were left uninfected (control) for 48 h. After infection, the medium was aspirated and cells were washed with 1 ml 1× PBS once. Three hundred microliters of 1× PBS-EDTA buffer was added per well for 5 to 10 min to help dissociate the cells from the well. The cells were transferred to 5-ml round-bottom tubes and washed twice in 1 ml of 1× PBS by centrifugation at 400 × *g* for 3 min. Cells were resuspended in 1 ml of 2% paraformaldehyde and fixed for 30 min at room temperature, followed by permeabilization in 500 μl Perm buffer (0.25% Tween 20 and 2% paraformaldehyde in 1× PBS). The cells were washed three times in FACS buffer (5% fetal bovine serum [FBS] and 0.02% NaN_3 in 1× PBS). Staining was performed in a 96-well round-bottom plate. The VSV-infected cells were stained in 50 μl of VSV G mouse monoclonal antibody I1 (38) or 50 μl of HeV G mouse monoclonal antibody 41C3 in FACS buffer for 30 min at room temperature. The RABV-infected cells were stained in 50 μl of the primary antibody mixture containing the RABV G human monoclonal antibody 4C12 and the HeV G mouse monoclonal antibody 41C3 in FACS buffer for 30 min at room temperature. This was followed by washing the cells twice in 200 μl FACS buffer. The VSV-infected cells were stained in 50 μl of donkey anti-mouse IgG conjugated to Cy3 in FACS buffer for 30 min at room temperature, whereas the RABV-infected cells were stained in 50 μl of a secondary antibody mixture of donkey anti-human IgG DyLight 649 and donkey anti-mouse IgG conjugated to Cy3 in FACS buffer for 30 min at room temperature, followed by being washed twice with 200 μl FACS buffer. VSV-infected cells were analyzed for Cy3 emission to detect VSV G or HeV G in the PE-Texas Red channel using a BD LSRII. The RABV-infected cells were analyzed for Cy3 emission to detect HeV G in the phycoerythrin (PE)-Texas Red channel and DyLight 649 emission to detect RABV G in the allophycocyanin (APC) channel using a BD LSRII. Data analysis was performed using FloJo software (Treestar, Ashland, OR).

Pathogenicity and immunogenicity studies. (i) Animal ethics statement. This study was carried out in strict adherence to recommendations described in the *Guide for the Care and Use of Laboratory Animals* (39), as well as guidelines of the National Institutes of Health, the Office of Animal Welfare, and the United States Department of Agriculture. All animal work was approved by the Institutional Animal Care and Use Committee (IACUC) at Thomas Jefferson University (animal protocols 414I and 414N). All procedures were carried out under isoflurane anesthesia by trained personnel, under the supervision of veterinary staff. Mice were housed in cages, in groups of five, under controlled conditions of humidity, temperature, and light (12-h light/12-h dark cycles). Food and water were available *ad libitum*.

(ii) Pathogenicity experiments. Five groups of five 6- to 8-week-old Swiss Webster mice were intranasally (i.n.) infected with 10^5 PFU (VSV) or focus-forming units (FFU) (RABV) of the live viruses diluted in 20 μl phosphate-buffered saline (PBS). The mice were weighed daily and monitored for signs of disease until day 28 postinfection. Mice that lost more than 20% weight were euthanized.

(iii) Immunizations. Ten groups of five 6- to 8-week-old BALB/c mice were immunized intramuscularly (i.m.) with 10^6 PFU or FFU of live virus, or 10 μg BPL-inactivated virus (3 doses at 0, 14, and 28 days) (see Fig. 4). All i.m. immunizations were performed by administering 50 μl of live or BPL-inactivated virus into each hind leg muscle. For serum collection, retro-orbital bleeds were performed under isoflurane anasthesia on days 0, 7, 14, 21, 28, and 35, with the final bleed on day 87. Sera from individual mice as well as pooled sera were analyzed for HeV G, RABV G, and VSV G IgG responses.

(iv) Production of HA-tagged HeV G. Subconfluent T175 flasks of 293T cells (human kidney cell line) were transfected with a pDisplay vector encoding amino acids 71 to 604 of the globular head and the stalk domains of the HeV G fused to an N-terminal hemagglutinin (HA) peptide. Supernatant was collected between days 5 to 7 posttransfection and loaded onto an equilibrated anti-HA agarose (Pierce) column containing a 2.5-ml agarose bed volume. The column was washed with 10 bed volumes of TBST (TBS containing 0.05% Tween 20) and 2 bed volumes of TBS. After 2 h of incubation at room temperature, antibody-bound HeV G was eluted with 5 ml of 250 μg/ml HA peptide in TBS. Fractions were collected and analyzed for HeV G by Western blotting with monoclonal anti-HA antibody (Sigma) prepared in 5% BSA–TBST. Peak fractions were then pooled and dialyzed against PBS in 10,000 molecular weight cutoff (MWCO) dialysis cassettes (Thermo Scientific) to remove excess HA peptide. After dialysis, the protein was quantitated by UV spectrophotometry and frozen in small aliquots at −80°C.

(v) Analysis of immune response to immunization. We tested individual mouse sera as well as pooled sera by enzyme-linked immunosorbent assay (ELISA) for the presence of IgG specific to HeV G, RABV G, and VSV G. In order to test for anti-HeV G humoral responses, we produced soluble HeV G (sHeV G) as described above. sHeV G was resuspended in coating buffer (50 mM Na_2CO_3 [pH 9.6]) at a concentration of 500 ng/ml and then plated in 96-well ELISA MaxiSorp plates (Nunc) at 100 μl in each well. RABV G and VSV G were similarly resuspended in coating buffer (50 mM Na_2CO_3 [pH 9.6]) at a concentration of 1 μg/ml and then plated in 96-well ELISA MaxiSorp plates (Nunc) at 100 μl per well. After overnight incubation at 4°C, plates were washed three times with PBST (0.05% Tween 20 in 1× PBS), which was followed by the addition of 250 μl blocking buffer (5% dry milk powder in 1× PBST) and incubation at room temperature for 1 h. The plates were then washed three times with PBST and incubated overnight at 4°C with serial dilutions of sera in PBS containing 0.5% BSA. Plates were washed three times the next day, followed by the addition of horseradish peroxidase-conjugated goat anti-mouse-IgG (H+L) secondary antibody (1:20,000) (Jackson ImmunoResearch). After incubation for 2 h at room temperature, plates were washed three times with PBST, and 200 μl of *o*-phenylenediamine dihydrochloride (OPD) substrate (Sigma) was added to each well. The reaction was stopped by the addition of 50 μl of 3 M H_2SO_4 per well. Optical density was determined at 490 nm (OD_{490}). IgG subclass-specific enzyme-linked immunosorbent assays (ELISAs) were performed for HeV G utilizing pooled sera (day 35) as described above for analysis of total anti-HeVG IgG. Three-fold serial dilutions of sera were prepared starting at a 1:150 dilution. Secondary antibodies specific for mouse IgG1 and IgG2a were diluted 1:2,000 or 1:20,000, respectively, in PBST, and 100 μl was added per well. Plates were incubated for 10 min with OPD substrate before the reaction was stopped with 3 M H_2SO_4. ELISA data were analyzed with GraphPad Prism using a sigmoidal nonlinear fit model to determine the titer at which the curves reach 50% of the top plateau value (50% effective concentration [EC_{50}]).

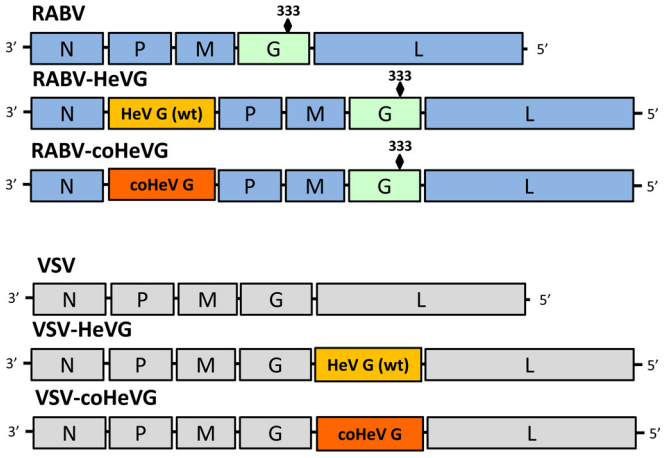

FIG 1 RABV- and VSV-based vaccine vectors. Shown is a schematic representation of the parental vectors (RABV and VSV) and the vaccine constructs expressing wild-type HeV G [RABV-HeVG (wt) and VSV-HeVG (wt)] or codon-optimized HeV G (RABV-coHeVG and VSV-coHeVG).

Virus neutralization assays against HeV and NiV. We prepared a 2-fold dilution series of the mouse serum samples starting at 1:10 in Dulbecco's modified Eagle's medium (DMEM)–2% FBS. HeV and NiV (Bangladesh isolate) were diluted in DMEM–2% FBS, achieving a final titer of 2,000 $TCID_{50}$/ml. Fifty microliters of virus (100 50% tissue culture infective doses [$TCID_{50}$]) was then incubated with 50 μl serum (day 85, heat inactivated) dilution for 60 min at 37°C. The virus-serum mixture was then added to a 96-well plate confluent with Vero cells and incubated for 3 days (NiV) or 5 days (HeV) at 37°C. Cytopathic effect (CPE) was recorded, and the lowest serum dilution at which no CPE on the Vero cells was detected was recorded as the virus neutralizing titer.

RESULTS

Rescue of recombinant viruses. The so-called "BNSP" RABV vaccine vector is derived from the RABV SAD B19 vaccine strain, which was attenuated by tissue culture passage (27, 30). The construct was engineered to contain an additional RABV stop-start transcription signal sequence flanked by unique BsiWI and NheI restriction sites between the nucleoprotein (N) and phosphoprotein (P) genes for introduction of foreign genes (Fig. 1). While BNSP is avirulent after peripheral administration in mice, it retains neurovirulence after intracerebral inoculation (40). There-

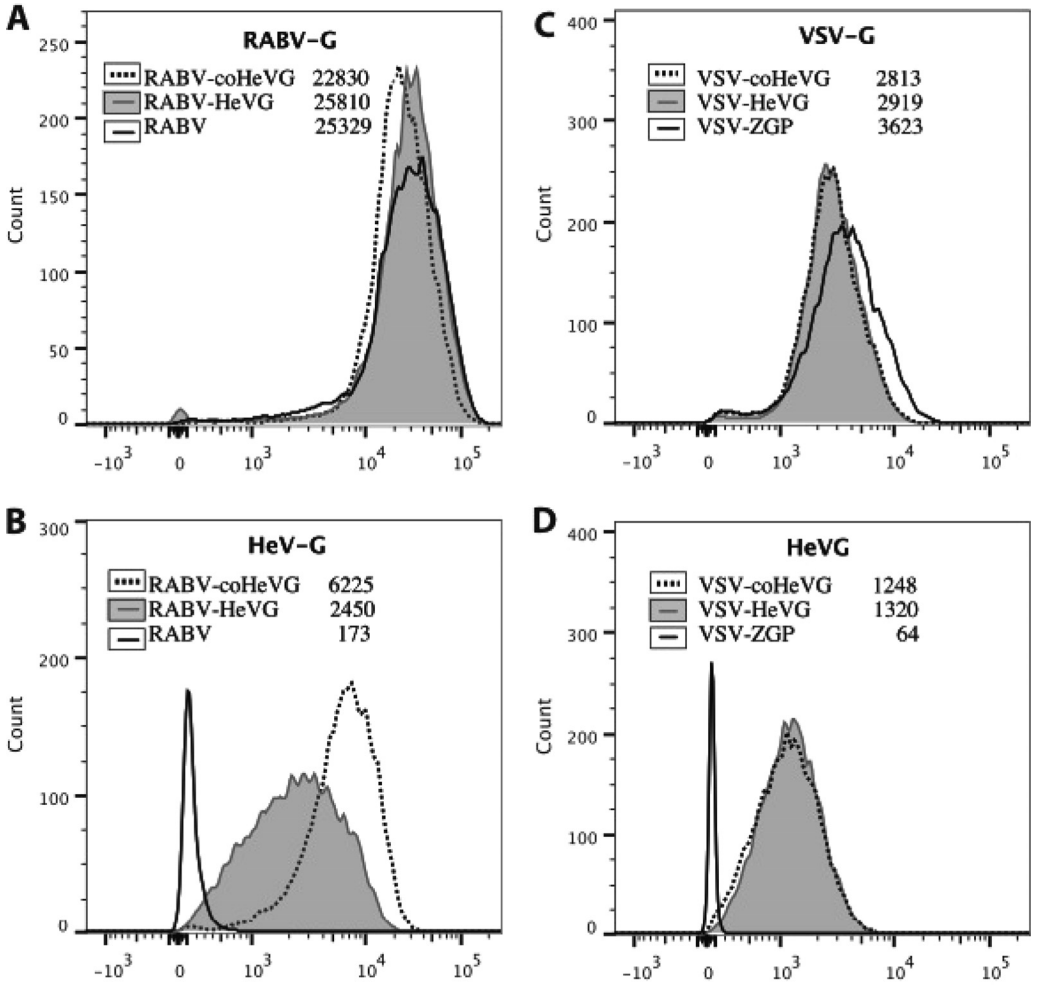

FIG 2 FACS analysis of expression of viral glycoproteins. Vero cells were infected with the recombinant RABVs or VSVs as indicated. Forty-eight hours (RABV) or 6.5 h (VSV) after infection, cells were stained with antibodies directed against RABV G, VSV G, or HeV G, as indicated, and analyzed by FACS. The numbers indicate the mean fluorescence intensity (MFI) for each staining.

fore, a further-attenuated derivative, BNSP333, was generated that contained an Arg→Glu change at amino acid 333 of the RABV G (31, 41). Studies in adult mice showed that this 333 mutation greatly reduced the neurovirulence observed with previous RABV vaccine vectors (28, 34, 40, 42).

The recombinant VSV (rVSV) vector VSV-XN, initially developed by Schnell et al. (35), is based on an infectious cDNA clone of the VSV Indiana serotype (32). It was modified by introducing a stop-start transcription signal sequence flanked by unique XhoI and NheI restriction sites between the glycoprotein (G) and large polymerase protein (L) genes for introduction of foreign genes (35). rVSV has been used to develop immunization strategies against a large number of pathogens, including influenza virus (43), Ebola virus (EBOV) (44), and human immunodeficiency virus (HIV) (45).

The goal of this study was to compare immunogenicity and safety in a small animal model of the two rhabdoviral vector platforms expressing the same foreign antigen. In order to generate the rRABV and rVSV vaccines expressing either wt or codon-optimized HeV G (coHeV G), we amplified the respective HeV G open reading frames (ORF) and inserted them into the RABV vector downstream of the RABV N gene between the BsiWI and NheI sites. We generated the rVSV vectors similarly, by amplifying the two respective HeV G ORFs and then inserting them into the plasmid downstream of the VSV G gene using the XhoI and the NheI sites. We recovered recombinant vaccine vectors RABV-HeVG, RABV-coHeVG, VSV-HeVG, and VSV-coHeVG by standard methods as described in Materials and Methods (46–49).

Characterization of recombinant viruses. Next, we wanted to determine the expression levels of HeV G and analyze the effects of codon optimization on HeV G expression and incorporation into virions for the four different vectors. For this approach, we infected different cell lines with RABV-HeVG, RABV-coHeVG, or the RABV control for 48 h or VSV-HeVG, VSV-coHeV, or the VSV-ZGP control for 6.5 h. Cells were then harvested, fixed, and stained with an antibody directed against HeV G, RABV G, or VSV G and analyzed by FACS. The results (Vero cells) are shown in Fig. 2. For the RABV-based constructs (RABV-HeVG and RABV-coHeVG), the detected expression level for coHeV G was about 2.5-fold higher than that for wt HeV G (Fig. 2A). In contrast, no significant difference was detected in HeV G expression for the two VSV constructs (VSV-HeVG and VSV-coHeVG) (Fig. 2B).

In the next step, we analyzed purified virions from BSR, 293T, or Vero cells infected with the four viruses by 10% SDS-PAGE. When we evaluated the SYPRO Ruby-stained gels, we found that HeV G incorporation was highest in Vero cell-derived virions, less in the BSR cell-derived virions, and lowest in 293T cell-derived virions for both RABV and VSV for both wt and coHeV G (data not shown). As shown in Fig. 3A (Vero cell-derived virions), a prominent monomeric protein band of ~80 kDa was detected in all the vaccine vectors expressing HeV G. Interestingly, we initially observed a less prominent band migrating above the 220-kDa marker for the four recombinant viruses expressing HeV G. This was similar to the results previously shown by Bossart et al. (15), wherein they showed a tetrameric band of partially reduced HeV G. This band disappeared after prolonged heating in reducing sample buffer (Fig. 3A). Western blot analysis of sucrose-purified virus particles confirmed that the additional ~80-kDa band is HeV G (Fig. 3B). The quantification results of the SYPRO Ruby-stained gels showed that HeV G incorporation was 2.5 to 3.5 times

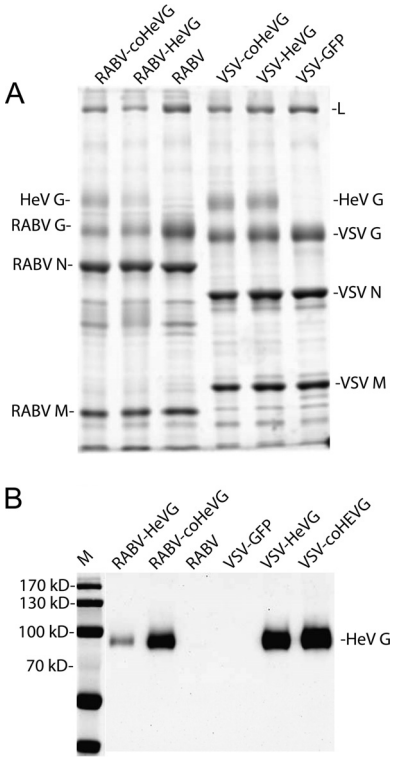

FIG 3 Analysis of purified virions of vaccine vectors. Purified virions (Vero cell derived) from RABV-coHeVG, RABV-HeVG, RABV, VSV-coHeVG, VSV-HeVG, or VSV-GFP were separated by SDS-PAGE and stained with SYPRO Ruby for total protein analysis (A) or transferred to a nitrocellulose membrane, and HeV G was detected by Western blotting (B). Lane M, molecular mass markers.

higher in RABV-coHeVG virions than RABV-HeVG virions. Notably we observed a slight increase in incorporation level at later harvests of the RABV-coHeVG virus with a concomitant slight reduction in RABV G levels (data not shown). We only obtained small differences for HeV G incorporation comparing VSV-coHeVG to VSV-HeVG (e.g., ~10% more [data not shown]), a finding that was consistent with the similar expression levels of the two proteins as detected by FACS. When we compared VSV-coHeVG and RABV-coHeVG, we observed a 70% increased incorporation of HeV G into VSV particles.

Incorporation of HeV G into RABV or VSV does not change vector pathogenicity. Both RABV and VSV vectors utilized in this study are highly attenuated. However, HeV G is known to bind to receptors that are present on neuronal cells, which could potentially restore the neurotropism of the RABV and/or VSV vectors and make them more pathogenic than the parental strains. To study the pathogenicity of the vaccine vectors, five groups of five Swiss Webster mice were infected intranasally (i.n.) with 1×10^5 plaque-forming units (PFU) of the live viruses and monitored for 28 days. The introduction and expression of HeV G into both vectors (VSV-coHeVG and RABV-coHeVG) did not result in any increase in pathogenicity, as indicated by the lack of clinical symptoms or weight loss in the infected mice (Fig. 4). There was also no pathogenicity observed with the control vector expressing Ebola (Zaire) virus glycoprotein (ZEBOV-GP) (BNSP333-ZGP in Fig. 4) (40), whereas all mice infected with the neurotropic control

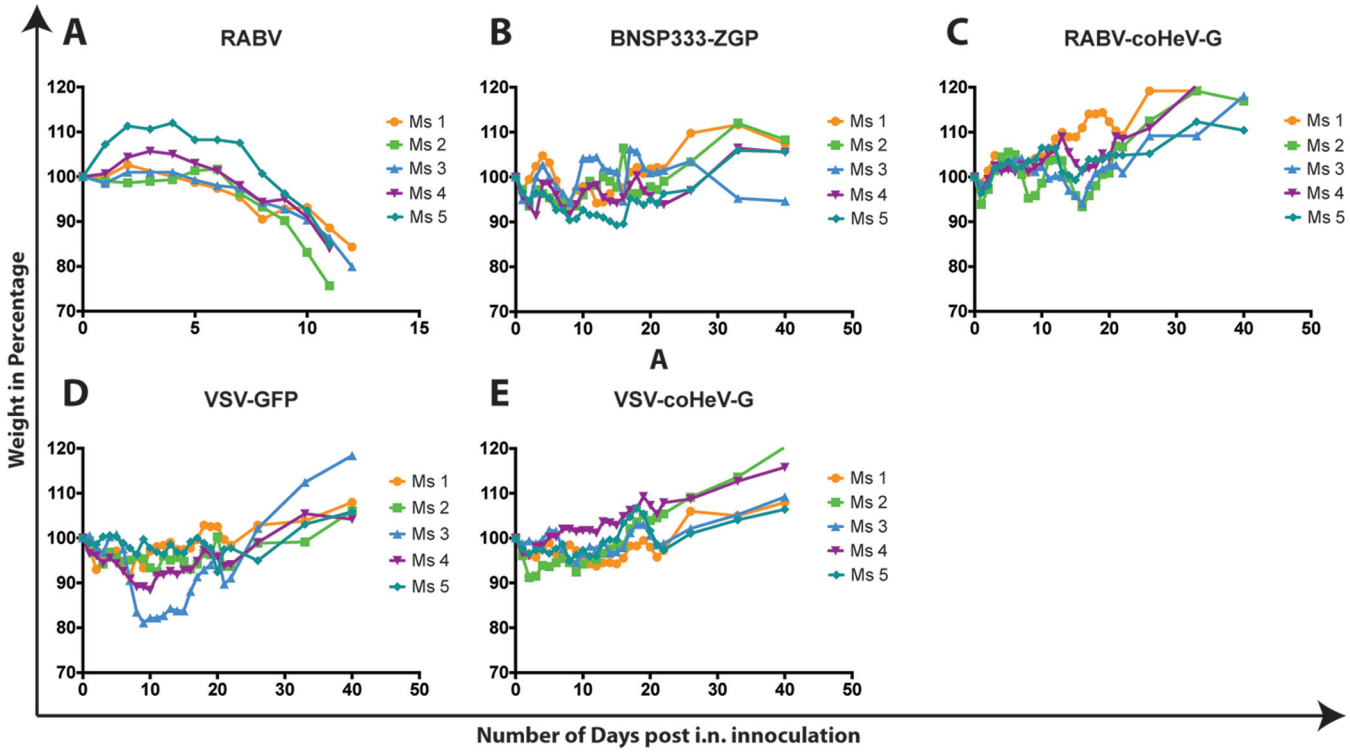

FIG 4 Pathogenicity study in Swiss Webster mice. Shown are weight curves of infected mice (Ms 1 to Ms 5) after i.n. inoculation with 10^5 PFU VSV or 10^5 FFU RABV live virus as indicated.

RABV vector BNSP succumbed to infection; this was previously shown by McGettigan et al. (28). Furthermore, we observed residual pathogenicity (weight loss) for infection with the control vector expressing green fluorescent protein, VSV-GFP (Fig. 4).

Immune responses to the vaccines. The goal of this study was to measure antibody responses against HeV G of the two different vaccine vectors based on RABV or VSV, to compare live and inactivated vaccines (3 doses), and to determine whether the vectors can be further improved by utilizing codon optimization of the viral antigen. We assessed the humoral immune response to vaccination in a BALB/c mouse model immunized intramuscularly with live or inactivated RABV or VSV (Fig. 5) over a period of 35 days.

Immunogenicity against HeV G. To analyze the HeV G-specific humoral responses, we purified the HA-tagged ectodomain of HeV G (sHeV G) from the supernatant of transiently transfected 293T cells by affinity column purification. We used the purified sHeV G to coat ELISA plates, as outlined in Materials and Methods, and analyzed sera from the immunized mice for the presence of HeV G-specific antibodies. The results in Fig. 6 indicate that seroconversion against HeV G occurred as early as day 7 after vaccination with the BPL-inactivated RABV [RABV-HeVG (BPL), RABV-coHeVG (BPL)] and all VSV-based vectors (live and BPL inactivated). In contrast, the anti-HeV G humoral responses induced by the live RABV vectors were close to the background level for both the wt HeV G and for the RABV-coHeVG vaccines. We observed no HeV G-specific responses for the controls (live and killed RABV vaccine without the HeV G insert) (Fig. 6) (data not shown).

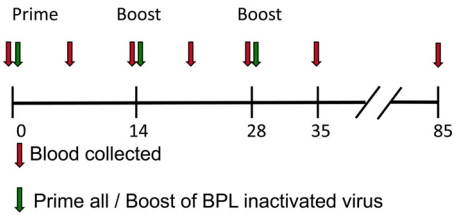

FIG 5 Experimental timeline of immunization study. BALB/c mice were immunized with either one dose of 10^5 PFU of live virus (day 0) or 3 doses of 10 μg inactivated virus (days 0, 14, and 28). Serum was collected every 7 days until day 35 and analyzed by ELISA. Final serum samples were collected on day 85 and used for determination of antibody neutralization titers.

HeV G-specific humoral responses were detectable on day 14 at similar levels for all VSV-based vaccines (live and BPL inactivated) and lower, but significant immune responses for the RABV-based vaccines. Interestingly, codon-optimized HeV G increased HeV G-specific immunity for both live and inactivated RABV vaccines (Fig. 6).

There was a large increase in the HeV G-specific IgG titers on day 21, 7 days after the first boost on day 14 with the inactivated viruses. The highest increase was measured for the VSV-coHevG BPL-inactivated vaccine, followed by the RABV-coHeVG BPL-inactivated vaccine. The RABV-HeVG BPL-inactivated vaccine induced a higher HeV G-specific IgG titer on day 21 compared to day 14, yet a lower IgG response in comparison to the coHeV G-expressing vaccines. The IgG titers for HeVG increased slightly from day 21 to day 35 for all of the BPL-inactivated vaccines after the second boost on day 28. On days 28 and 35, the HeV G-specific IgG titers were the highest for the BPL-inactivated VSV-coHeVG

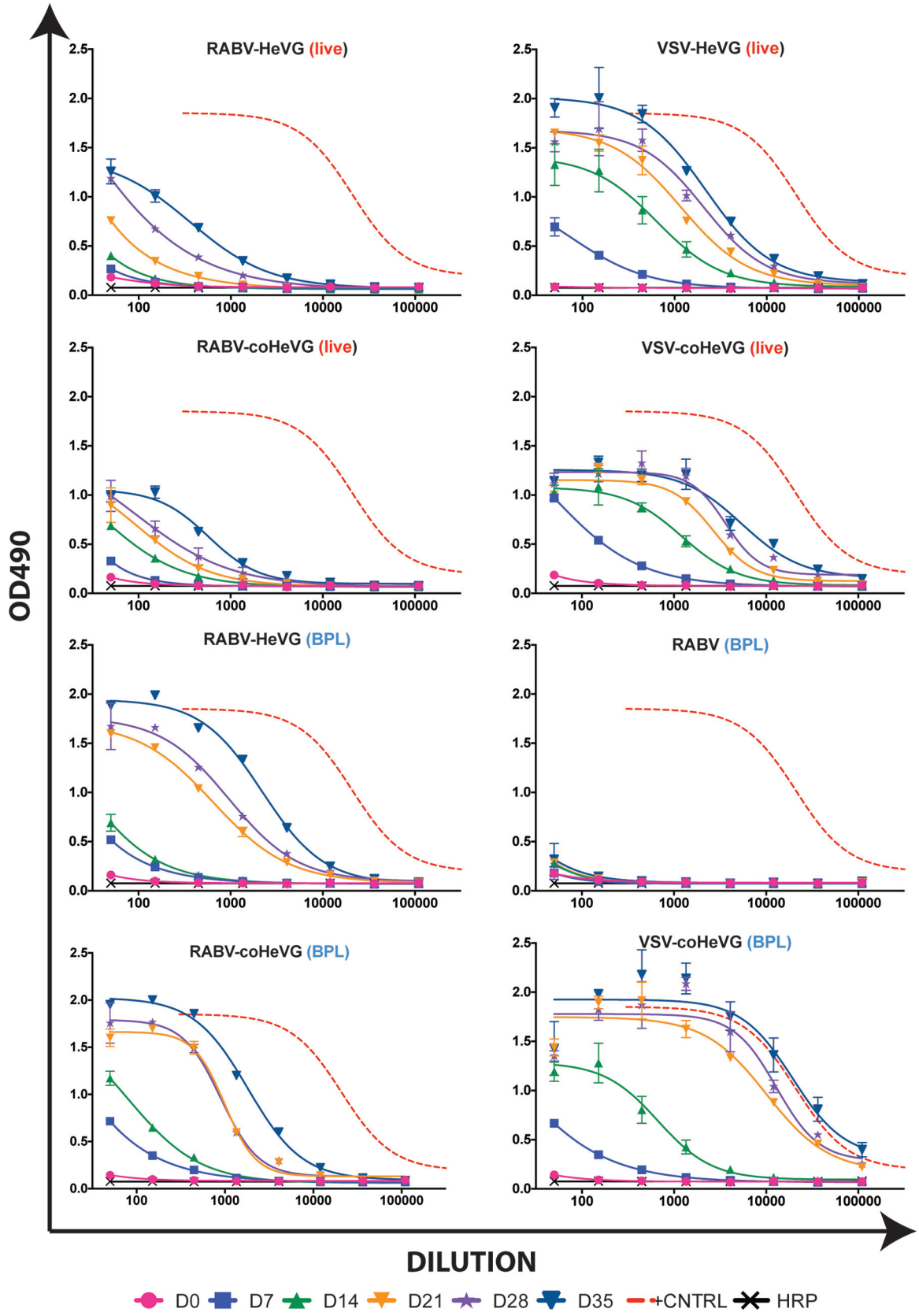

FIG 6 Analysis of anti-HeV G humoral immune response of immunized mice. BALB/c mice were immunized as indicated in the legend to Fig. 5, and blood was collected on days 0, 7, 14, 21, 28, and 35. Serum was pooled from each group and analyzed for total IgG against HeV G by ELISA. All sera were diluted 1:50 and analyzed in 3-fold dilutions; the error bars indicate the standard deviations of the samples analyzed in triplicates. The nonlinear curve fit of the group with the highest titer (BPL-inactivated VSV-coHeVG at day 35 postimmunization) is shown as a red dotted curve in all graphs for comparative reference. OD490, optical density at 490 nm.

TABLE 1 Virus neutralization assay and endpoint titer results from sera at day 85 postimmunization

Vaccine construct	HeV G endpoint titer (ELISA)	VNA titer	
		HeV	NiV
RABV-HeVG	109,000	1:120	NN[a]
RABV-coHeVG	109,000	1:60	NN
RABV-HeVG inactivated	984,150	1:480	NN
RABV-coHeVG inactivated	984,150	1:1,280	1:40
VSV-HeVG	984,150	1:640	1:10
VSV-coHeVG	984,150	1:960	1:160
VSV-coHeVG inactivated	2,952,450	1:1,920	1:80
RABV	1,350	NN	NN
RABV inactivated	1,350	NN	NN
PBS	1,350	NN	NN

[a] NN, nonneutralizing antibodies.

vaccine, followed by the BPL-inactivated RABV-coHeVG and RABV-HeVG vaccines.

In summary, the administration of three doses of BPL-inactivated vaccines induced a higher anti-HeV G-specific IgG response than a single dose of live vaccines for the RABV- and VSV-based vectors. Among the live vaccines, the total IgG response against HeV G was highest for the VSV live vaccine (endpoint titer, 1:984,150) and about 10-fold less for the vaccines RABV-coHeVG and RABV-HeVG (endpoint titer, 1:109,000) (Table 1). Among the killed particle-based vaccines, endpoint titers were more similar for VSV and RABV (Table 1). Notably, the final titer for both the live and the killed RABV-based vaccine vectors was unaffected by the codon optimization of HeV G. However, the HeV G-specific total IgG response developed faster for all RABV-coHeVG-based vaccines. Also, we noted qualitative antibody differences between the wt HeVG and coHeVG vectors, as indicated below.

HeV and NiV neutralization assays. To analyze the potency of the final sera (day 85) of the immunized mice, we performed a virus neutralization assay (VNA) against HeV and NiV. Sera from all mice immunized with killed or live HeV G vaccines induced VNA against Hendra virus (Table 1). The ELISA titers correlated to some extent with the neutralization titers, with less-pronounced differences in the HeV G-specific ELISA. For example, the VNA titers for the killed particles were very similar for RABV and VSV, whereas the ELISA titers were 3-fold different. As a general trend, high neutralization titers against HeV also provided some cross-neutralization against NiV, whereas the lower titers did not provide any neutralizing activity against the heterologous virus.

Antibody quality. Antibody quality can play an important role in protecting the infected host. Therefore, we further analyzed the composition of the total anti-HeVG IgG for IgG1 versus IgG2a classes. As shown in Fig. 7, the IgG responses were mostly Th1 biased (IgG2a). The lack of detectable IgG1 was most notable for the two live RABV vectors. It was less pronounced for the live VSV vectors, even though we also observed a Th1 bias with a IgG2a/IgG1 ratio of 2. Interestingly, it appears that the higher incorporation rate of coHeV G into RABV virions also skewed the immune response toward Th1 as seen for the sera from mice immunized with killed particles of RABV-HeVG compared to RABV-coHeVG. Further experiments are needed to analyze whether the differences in isotype bias for the different vaccines also affect differences in protection, as proposed for other viruses, such as EBOV.

RABV and VSV G response. In order to determine the vector-specific immune response, we also analyzed the humoral responses to RABV G and VSV G, respectively (Fig. 8A and B). We observed that the administration of three doses of BPL-inactivated virus particles induced a higher vector-specific response than one dose of live virus. The difference was quite significant for the RABV vaccines but much smaller for the VSV vaccines. Among the live RABV vaccines, no significant difference was observed between the parental RABV vector and the RABV vaccines expressing wt or coHeV G. However, among the BPL-inactivated RABV vectors, a slight decrease in vector-specific immune response was seen for the RABV-coHeVG vaccine compared to the parental vector. This result indicated that the incorporation of a foreign protein into the virion membrane can interfere with RABV G-specific immunity.

DISCUSSION

The high mortality rate of both HeV and NiV infections in humans, in combination with the frequent spillovers observed in recent years, has raised interest in a vaccine against henipaviruses for human use. In the past decade, researchers have developed multiple vaccine and monoclonal antibody approaches against henipaviruses and tested them in animal models (15, 16, 18, 24, 25, 50). However, only one of the candidate vaccines, an HeV subunit vaccine for immunization of horses, has been licensed to date (50). In this study, we evaluated and compared the immunogenicities of two well-established rhabdoviral platforms expressing HeV G in a mouse model. The decision to use VSV and RABV vectors was based on their excellent safety record and their ability to induce neutralizing antibody responses against other viral pathogens (28, 34, 40, 45, 46, 48, 51, 52). We performed this study with the ultimate goal of developing a vaccine for use in humans and animals. We also wanted to compare VSV and RABV vectors in parallel, which has not been done before.

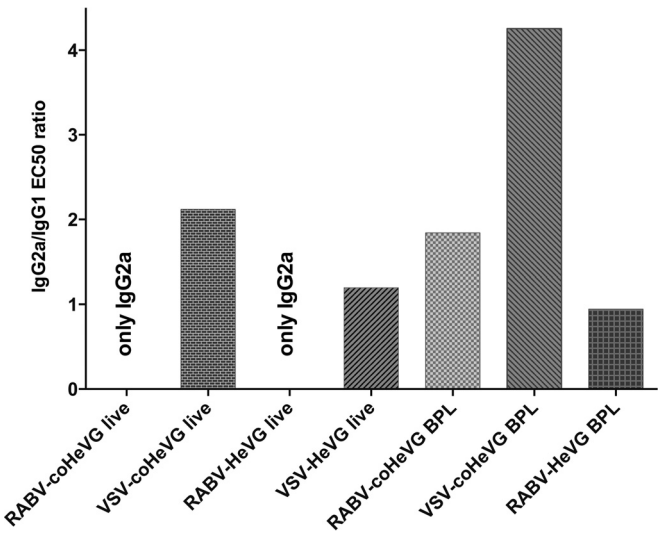

FIG 7 Anti-HeVG IgG isotype analysis of immunized mice. Serum from BALB/c mice collected 35 days after immunization (see Fig. 5) was analyzed for the presence of anti-HeVG IgG1 and IgG2a by ELISA. The graph shows the IgG2a/IgG1 EC_{50} ratio of the sera.

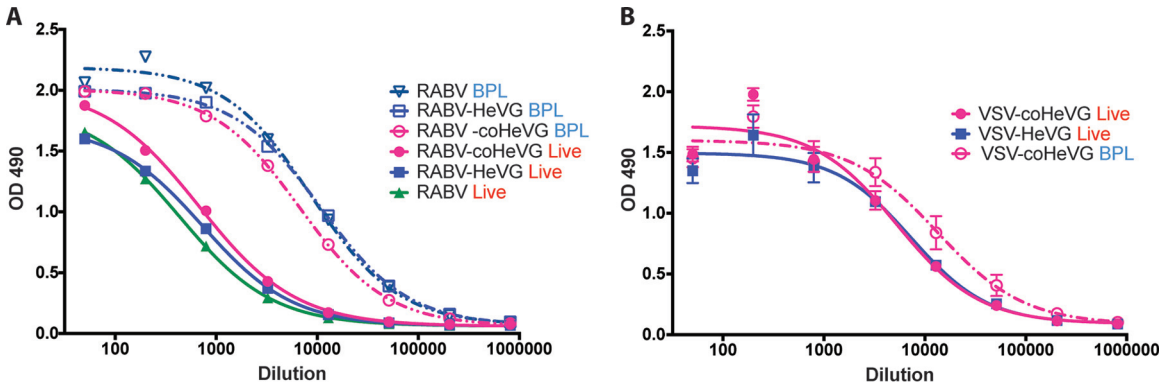

FIG 8 Humoral vector response to RABV G or VSV G. Total IgG to RABV G (A) or VSV G (B) was determined from the sera collected at day 35 after immunization with the different vaccines. All sera were diluted 1:50 and analyzed in 3-fold dilutions specific for RABV G (A) or VSV G (B). The error bars indicate the standard deviations of the samples analyzed in triplicates.

In agreement with previous studies, we observed efficient incorporation of HeV G into RABV and VSV particles. Numerous studies have shown that both RABV and VSV can incorporate foreign glycoproteins into their envelope (for a review, see references 33 and 41). Incorporation levels can vary widely from nearly undetectable levels in the case of cellular receptor proteins (53, 54) to more than 10% of total glycoprotein in the case of other viral envelope proteins (43, 49). The latter do not generally require the presence of a rhabdovirus-specific incorporation signal (49). This was demonstrated by the efficient pseudotyping of VSV with several viral glycoproteins, including HeV G (55, 56). In other studies, RABV vectors efficiently incorporated ZEBOV GP (40) and hepatitis C virus E2 (57) in the presence or absence of RABV G. Also, ZEBOV GP incorporation was not dependent on or enhanced by the exchange of the GP transmembrane (TM) domain with that of the RABV G TM domain (40), whereas efficient incorporation of CD4 and CXCR4 depended on the presence of the RABV G cytoplasmic tail (54). This difference most likely occurs because certain viral glycoproteins already harbor transport signals that direct them to common viral budding sites. In contrast, the cellular receptors CD4 and CXCR4 lack these signals and are targeted to different intracellular locations, as shown for VSV (58). Taken together, these studies indicate that rhabdoviruses can incorporate foreign glycoproteins indiscriminately, provided they are present at sufficient levels at the budding site.

Based on this conclusion, we hypothesized that codon optimization would result in a higher protein expression and consequently a higher level of HeV G incorporation into virions. This proved to be true for the recombinant RABV vectors but not for the recombinant VSVs. The reasons for this difference are unclear, but the difference could be caused by the faster transport of VSV G (59) compared to RABV G (60), the rapid replication cycle of VSV, or the fast shutoff of host protein translation in VSV-infected cells.

Even though the incorporation levels achieved with the vectors described here are sufficient to induce strong humoral immune responses against HeV G, it might be worth exploring other ways to increase incorporation levels. For instance, pseudotyping of lentiviral particles with HeV G can be made more efficient if the cytoplasmic tail of G is truncated (55, 61). The same strategy might also improve incorporation into VSV and RABV particles.

In addition to being immunogenic and efficacious against their target pathogen, vaccine candidates need to be proven safe. Although the RABV and VSV vectors used here were previously shown to be safe, it is possible that the addition of HeV G could have restored the neurotropism of the vectors and made them more pathogenic than the parental vectors, since HeV itself is neurotropic and able to bind to a highly conserved receptor on neuronal cells (10). The results of the pathogenicity experiment indicated that this is not the case and that the vaccines are still attenuated, which confirmed the excellent safety profile of the VSV and RABV vectors in numerous previous studies. However, further studies would be needed to confirm that they are apathogenic and safe for human use (62). Of note, killed viral particles are always considered safer because they cannot replicate.

The findings of this study indicate that live VSV vectors induce higher immune responses against HeV G than live RABV vectors. We have hypothesized that this is due to the faster viral replication cycle of VSV, which causes very high viral loads early in infection and therefore induces an anti-HeV G response before the vector can be neutralized. Conversely, RABV is a slow-growing virus that is likely neutralized before it can induce such high anti-HeV G humoral responses. Since the immune responses against foreign glycoproteins, such as ZEBOV GP, have been shown to be protective (34, 40), the next step needs to be a challenge experiment to analyze the protective parameter of such antibodies against HeV.

We also showed that BPL-inactivated rhabdoviral particles induced higher antibody titers than the live vaccines with the highest antibody titers detected for VSV-based particles. We speculate that the reason for the higher induction of HeV G-specific immune responses by BPL-inactivated VSV-coHeVG particles compared to RABV-inactivated virions could be due to the different receptor usage by VSV G versus RABV G. This difference could influence the efficiency of uptake by dendritic cells, macrophages, or other antigen-presenting cells. However, the VNA results were only modestly different for the inactivated RABV and VSV vaccines expressing codon-optimized HeV G. Therefore, BPL-inactivated RABV particles are the vaccine of choice based on the availability of a production line and the advantage of a dual vaccine providing protection against RABV in addition to HeV. In addition, the inactivated particles can be administered multiple times to boost their immunogenicity. This is not possible for the live vaccines due to the antivector immunity induced after the first

inoculation and certainly explains the lower antibody titers elicited by the live viruses compared to the BPL-treated particles.

Th1-biased immune responses are generally considered beneficial against viral infections. Previous studies by others have indicated that BALB/c mice, which we also utilized in our study, have a predisposition for mounting a Th2-biased immune response (63). Hence, we conclude that the Th1-biased response we observed in the immunized mice should most likely be similarly induced in other species. Interestingly, the codon optimization of HeV G increased the Th1-biased responses for both VSV and RABV. This observation warrants further studies to determine whether similar changes in antibody quality can be replicated with rhabdoviral vectors expressing other viral glycoproteins.

ACKNOWLEDGMENTS

This work was supported in part by the NIAID Division of Intramural Research, NIAID grant R01AI105204 to M.J.S., and the Jefferson Vaccine Center.

We thank C. C. Broder (Uniformed Services University, Bethesda, MD), John Rose (Yale University, New Haven, CT), and Scott Dessain (Lankenau Institute for Medical Research, Wynnewood, PA) for the generous gifts of the mouse monoclonal antibody against HeV G, hybridomas producing monoclonal antibodies against VSV G, and human monoclonal antibody against RABV G, respectively. Hendra and Nipah viruses were kindly provided by the Viral Special Pathogens Branch, Centers for Disease Control and Prevention, Atlanta, GA. We thank Jennifer Wilson (Thomas Jefferson University, Philadelphia, PA) for critical readings and editing of the manuscript.

REFERENCES

1. **Eaton BT, Broder CC, Middleton D, Wang LF.** 2006. Hendra and Nipah viruses: different and dangerous. Nat Rev Microbiol **4:**23–35. http://dx.doi.org/10.1038/nrmicro1323.
2. **Lee B, Rota PA** 2012. Henipavirus—ecology, molecular virology, and pathogenesis. Curr Top Microbiol Immunol **359:**41–58. http://dx.doi.org/10.1007/82_2012_211.
3. **Hsu VP.** 2007. Emerging viruses in human populations—Nipah and Hendra viruses, vol 16. Elsevier, Amsterdam, The Netherlands.
4. **Marsh GA, Wang LF.** 2012. Hendra and Nipah viruses: why are they so deadly? Curr Opin Virol **2:**242–247. http://dx.doi.org/10.1016/j.coviro.2012.03.006.
5. **Field H, Young P, Yob JM, Mills J, Hall L, Mackenzie J.** 2001. The natural history of Hendra and Nipah viruses. Microbes Infect **3:**307–314. http://dx.doi.org/10.1016/S1286-4579(01)01384-3.
6. **Young PL, Halpin K, Selleck PW, Field H, Gravel JL, Kelly MA, Mackenzie JS.** 1996. Serologic evidence for the presence in Pteropus bats of a paramyxovirus related to equine morbillivirus. Emerg Infect Dis **2:**239–240. http://dx.doi.org/10.3201/eid0203.960315.
7. **Aljofan M.** 2013. Hendra and Nipah infection: emerging paramyxoviruses. Virus Res **177:**119–126. http://dx.doi.org/10.1016/j.virusres.2013.08.002.
8. **Mohd Nor MN, Gan CH, Ong BL.** 2000. Nipah virus infection of pigs in peninsular Malaysia. Rev. Sci Tech **19:**160–165.
9. **Steffen DL, Xu K, Nikolov DB, Broder CC.** 2012. Henipavirus mediated membrane fusion, virus entry and targeted therapeutics. Viruses **4:**280–308. http://dx.doi.org/10.3390/v4020280.
10. **Xu K, Broder CC, Nikolov DB.** 2012. Ephrin-B2 and ephrin-B3 as functional henipavirus receptors. Semin Cell Dev Biol **23:**116–123. http://dx.doi.org/10.1016/j.semcdb.2011.12.005.
11. **Mellitzer G, Xu Q, Wilkinson DG.** 1999. Eph receptors and ephrins restrict cell intermingling and communication. Nature **400:**77–81. http://dx.doi.org/10.1038/21907.
12. **Su Z, Xu P, Ni F.** 2004. Single phosphorylation of Tyr304 in the cytoplasmic tail of ephrin B2 confers high-affinity and bifunctional binding to both the SH2 domain of Grb4 and the PDZ domain of the PDZ-RGS3 protein. Eur J Biochem **271:**1725–1736. http://dx.doi.org/10.1111/j.1432-1033.2004.04078.x.
13. **Gale NW, Baluk P, Pan L, Kwan M, Holash J, DeChiara TM, McDonald DM, Yancopoulos GD.** 2001. Ephrin-B2 selectively marks arterial vessels and neovascularization sites in the adult, with expression in both endothelial and smooth-muscle cells. Dev Biol **230:**151–160. http://dx.doi.org/10.1006/dbio.2000.0112.
14. **Negrete OA, Chu D, Aguilar HC, Lee B.** 2007. Single amino acid changes in the Nipah and Hendra virus attachment glycoproteins distinguish ephrinB2 from ephrinB3 usage. J Virol **81:**10804–10814. http://dx.doi.org/10.1128/JVI.00999-07.
15. **Bossart KN, Crameri G, Dimitrov AS, Mungall BA, Feng YR, Patch JR, Choudhary A, Wang LF, Eaton BT, Broder CC.** 2005. Receptor binding, fusion inhibition, and induction of cross-reactive neutralizing antibodies by a soluble G glycoprotein of Hendra virus. J Virol **79:**6690–6702. http://dx.doi.org/10.1128/JVI.79.11.6690-6702.2005.
16. **Bossart KN, Zhu Z, Middleton D, Klippel J, Crameri G, Bingham J, McEachern JA, Green D, Hancock TJ, Chan YP, Hickey AC, Dimitrov DS, Wang LF, Broder CC.** 2009. A neutralizing human monoclonal antibody protects against lethal disease in a new ferret model of acute Nipah virus infection. PLoS Pathog **5:**e1000642. http://dx.doi.org/10.1371/journal.ppat.1000642.
17. **Prabakaran P, Zhu Z, Xiao X, Biragyn A, Dimitrov AS, Broder CC, Dimitrov DS.** 2009. Potent human monoclonal antibodies against SARS CoV, Nipah and Hendra viruses. Expert Opin Biol Ther **9:**355–368. http://dx.doi.org/10.1517/14712590902763755.
18. **Bossart KN, Geisbert TW, Feldmann H, Zhu Z, Feldmann F, Geisbert JB, Yan L, Feng YR, Brining D, Scott D, Wang Y, Dimitrov AS, Callison J, Chan YP, Hickey AC, Dimitrov DS, Broder CC, Rockx B.** 2011. A neutralizing human monoclonal antibody protects African green monkeys from Hendra virus challenge. Sci Transl Med 3:105ra103. http://dx.doi.org/10.1126/scitranslmed.3002901.
19. **Geisbert TW, Mire CE, Geisbert JB, Chan YP, Agans KN, Feldmann F, Fenton KA, Zhu Z, Dimitrov DS, Scott DP, Bossart KN, Feldmann H, Broder CC.** 2014. Therapeutic treatment of Nipah virus infection in nonhuman primates with a neutralizing human monoclonal antibody. Sci Transl Med 6:242ra282. http://dx.doi.org/10.1126/scitranslmed.3008929.
20. **DeBuysscher BL, Scott D, Marzi A, Prescott J, Feldmann H.** 2014. Single-dose live-attenuated Nipah virus vaccines confer complete protection by eliciting antibodies directed against surface glycoproteins. Vaccine **32:**2637–2644. http://dx.doi.org/10.1016/j.vaccine.2014.02.087.
21. **Mire CE, Versteeg KM, Cross RW, Agans KN, Fenton KA, Whitt MA, Geisbert TW.** 2013. Single injection recombinant vesicular stomatitis virus vaccines protect ferrets against lethal Nipah virus disease. Virol J **10:**353. http://dx.doi.org/10.1186/1743-422X-10-353.
22. **Lo MK, Bird BH, Chattopadhyay A, Drew CP, Martin BE, Coleman JD, Rose JK, Nichol ST, Spiropoulou CF.** 2014. Single-dose replication-defective VSV-based Nipah virus vaccines provide protection from lethal challenge in Syrian hamsters. Antiviral Res **101:**26–29. http://dx.doi.org/10.1016/j.antiviral.2013.10.012.
23. **Ploquin A, Szecsi J, Mathieu C, Guillaume V, Barateau V, Ong KC, Wong KT, Cosset FL, Horvat B, Salvetti A.** 2013. Protection against henipavirus infection by use of recombinant adeno-associated virus-vector vaccines. J Infect Dis **207:**469–478. http://dx.doi.org/10.1093/infdis/jis699.
24. **Mire CE, Geisbert JB, Agans KN, Feng YR, Fenton KA, Bossart KN, Yan L, Chan YP, Broder CC, Geisbert TW.** 2014. A recombinant Hendra virus G glycoprotein subunit vaccine protects nonhuman primates against Hendra virus challenge. J Virol **88:**4624–4631. http://dx.doi.org/10.1128/JVI.00005-14.
25. **Bossart KN, Rockx B, Feldmann F, Brining D, Scott D, LaCasse R, Geisbert JB, Feng YR, Chan YP, Hickey AC, Broder CC, Feldmann H, Geisbert TW.** 2012. A Hendra virus G glycoprotein subunit vaccine protects African green monkeys from Nipah virus challenge. Sci Transl Med 4:146ra107. http://dx.doi.org/10.1126/scitranslmed.3004241.
26. **Mendez D, Buttner P, Speare R.** 2013. Response of Australian veterinarians to the announcement of a Hendra virus vaccine becoming available. Aust Vet J **91:**328–331. http://dx.doi.org/10.1111/avj.12092.
27. **Vos A, Neubert A, Aylan O, Schuster P, Pommerening E, Muller T, Chivatsi DC.** 1999. An update on safety studies of SAD B19 rabies virus vaccine in target and non-target species. Epidemiol Infect **123:**165–175. http://dx.doi.org/10.1017/S0950268899002666.
28. **McGettigan JP, Pomerantz RJ, Siler CA, McKenna PM, Foley HD, Dietzschold B, Schnell MJ.** 2003. Second-generation rabies virus-based vaccine vectors expressing human immunodeficiency virus type 1 Gag

have greatly reduced pathogenicity but are highly immunogenic. J Virol **77:**237–244. http://dx.doi.org/10.1128/JVI.77.1.237-244.2003.
29. **Gomme EA, Wirblich C, Addya S, Rall GF, Schnell MJ.** 2012. Immune clearance of attenuated rabies virus results in neuronal survival with altered gene expression. PLoS Pathog **8:**e1002971. http://dx.doi.org/10.1371/journal.ppat.1002971.
30. **Schnell MJ, Foley HD, Siler CA, McGettigan JP, Dietzschold B, Pomerantz RJ.** 2000. Recombinant rabies virus as potential live-viral vaccines for HIV-1. Proc Natl Acad Sci U S A **97:**3544–3549. http://dx.doi.org/10.1073/pnas.97.7.3544.
31. **Dietzschold B, Wunner WH, Wiktor TJ, Lopes AD, Lafon M, Smith CL, Koprowski H.** 1983. Characterization of an antigenic determinant of the glycoprotein that correlates with pathogenicity of rabies virus. Proc Natl Acad Sci U S A **80:**70–74. http://dx.doi.org/10.1073/pnas.80.1.70.
32. **Lawson ND, Stillman EA, Whitt MA, Rose JK.** 1995. Recombinant vesicular stomatitis viruses from DNA. Proc Natl Acad Sci U S A **92:**4477–4481. http://dx.doi.org/10.1073/pnas.92.10.4477.
33. **Roberts A, Buonocore L, Price R, Forman J, Rose JK.** 1999. Attenuated vesicular stomatitis viruses as vaccine vectors. J Virol **73:**3723–3732.
34. **Blaney JE, Marzi A, Willet M, Papaneri AB, Wirblich C, Feldmann F, Holbrook M, Jahrling P, Feldmann H, Schnell MJ.** 2013. Antibody quality and protection from lethal Ebola virus challenge in nonhuman primates immunized with rabies virus based bivalent vaccine. PLoS Pathog **9:**e1003389. http://dx.doi.org/10.1371/journal.ppat.1003389.
35. **Schnell MJ, Buonocore L, Whitt MA, Rose JK.** 1996. The minimal conserved transcription stop-start signal promotes stable expression of a foreign gene in vesicular stomatitis virus. J Virol **70:**2318–2323.
36. **Harty RN, Brown ME, Hayes FP, Wright NT, Schnell MJ.** 2001. Vaccinia virus-free recovery of vesicular stomatitis virus. J Mol Microbiol Biotechnol **3:**513–517.
37. **Papaneri AB, Wirblich C, Marissen WE, Schnell MJ.** 2013. Alanine scanning of the rabies virus glycoprotein antigenic site III using recombinant rabies virus: implication for post-exposure treatment. Vaccine **31:**5897–5902. http://dx.doi.org/10.1016/j.vaccine.2013.09.038.
38. **Lefrancois L, Lyles DS.** 1982. The interaction of antibody with the major surface glycoprotein of vesicular stomatitis virus. I. Analysis of neutralizing epitopes with monoclonal antibodies. Virology **121:**157–167.
39. **National Research Council.**2011. Guide for the care and use of laboratory animals, 8th ed. National Academies Press, Washington, DC.
40. **Blaney JE, Wirblich C, Papaneri AB, Johnson RF, Myers CJ, Juelich TL, Holbrook MR, Freiberg AN, Bernbaum JG, Jahrling PB, Paragas J, Schnell MJ.** 2011. Inactivated or live-attenuated bivalent vaccines that confer protection against rabies and Ebola viruses. J Virol **85:**10605–10616. http://dx.doi.org/10.1128/JVI.00558-11.
41. **Gomme EA, Wanjalla CN, Wirblich C, Schnell MJ.** 2011. Rabies virus as a research tool and viral vaccine vector. Adv Virus Res **79:**139–164. http://dx.doi.org/10.1016/B978-0-12-387040-7.00009-3.
42. **Papaneri AB, Wirblich C, Cann JA, Cooper K, Jahrling PB, Schnell MJ, Blaney JE.** 2012. A replication-deficient rabies virus vaccine expressing Ebola virus glycoprotein is highly attenuated for neurovirulence. Virology **434:**18–26. http://dx.doi.org/10.1016/j.virol.2012.07.020.
43. **Kretzschmar E, Buonocore L, Schnell MJ, Rose JK.** 1997. High-efficiency incorporation of functional influenza virus glycoproteins into recombinant vesicular stomatitis viruses. J Virol **71:**5982–5989.
44. **Marzi A, Feldmann H, Geisbert TW, Falzarano D.** 2011. Vesicular stomatitis virus-based vaccines for prophylaxis and treatment of filovirus infections. J Bioterror Biodef **2011**(Suppl 1)**:**2157–2526-S1-004. http://dx.doi.org/10.4172/2157-2526.S1-004.
45. **Ramsburg E, Rose NF, Marx PA, Mefford M, Nixon DF, Moretto WJ, Montefiori D, Earl P, Moss B, Rose JK.** 2004. Highly effective control of an AIDS virus challenge in macaques by using vesicular stomatitis virus and modified vaccinia virus Ankara vaccine vectors in a single-boost protocol. J Virol **78:**3930–3940. http://dx.doi.org/10.1128/JVI.78.8.3930-3940.2004.
46. **Faber M, Lamirande EW, Roberts A, Rice AB, Koprowski H, Dietzschold B, Schnell MJ.** 2005. A single immunization with a rhabdovirus-based vector expressing severe acute respiratory syndrome coronavirus (SARS-CoV) S protein results in the production of high levels of SARS-CoV-neutralizing antibodies. J Gen Virol **86:**1435–1440. http://dx.doi.org/10.1099/vir.0.80844-0.
47. **McKenna PM, Koser ML, Carlson KR, Montefiori DC, Letvin NL, Papaneri AB, Pomerantz RJ, Dietzschold B, Silvera P, McGettigan JP, Schnell MJ.** 2007. Highly attenuated rabies virus-based vaccine vectors expressing simian-human immunodeficiency virus89.6P Env and simian immunodeficiency virus mac239 Gag are safe in rhesus macaques and protect from an AIDS-like disease. J Infect Dis **195:**980–988. http://dx.doi.org/10.1086/512243.
48. **Schell JB, Rose NF, Bahl K, Diller K, Buonocore L, Hunter M, Marx PA, Gambhira R, Tang H, Montefiori DC, Johnson WE, Rose JK.** 2011. Significant protection against high-dose simian immunodeficiency virus challenge conferred by a new prime-boost vaccine regimen. J Virol **85:**5764–5772. http://dx.doi.org/10.1128/JVI.00342-11.
49. **Schnell MJ, Buonocore L, Kretzschmar E, Johnson E, Rose JK.** 1996. Foreign glycoproteins expressed from recombinant vesicular stomatitis viruses are incorporated efficiently into virus particles. Proc Natl Acad Sci U S A **93:**11359–11365. http://dx.doi.org/10.1073/pnas.93.21.11359.
50. **Middleton D, Pallister J, Klein R, Feng YR, Haining J, Arkinstall R, Frazer L, Huang JA, Edwards N, Wareing M, Elhay M, Hashmi Z, Bingham J, Yamada M, Johnson D, White J, Foord A, Heine HG, Marsh GA, Broder CC, Wang LF.** 2014. Hendra virus vaccine, a one health approach to protecting horse, human, and environmental health. Emerg Infect Dis **20:**372–379. http://dx.doi.org/10.3201/eid2003.131159.
51. **Gomme EA, Faul EJ, Flomenberg P, McGettigan JP, Schnell MJ.** 2010. Characterization of a single-cycle rabies virus-based vaccine vector. J Virol **84:**2820–2831. http://dx.doi.org/10.1128/JVI.01870-09.
52. **Schwartz JA, Buonocore L, Suguitan A, Jr, Hunter M, Marx PA, Subbarao K, Rose JK.** 2011. Vesicular stomatitis virus-based H5N1 avian influenza vaccines induce potent cross-clade neutralizing antibodies in rhesus macaques. J Virol **85:**4602–4605. http://dx.doi.org/10.1128/JVI.02491-10.
53. **Johnson JE, Schnell MJ, Buonocore L, Rose JK.** 1997. Specific targeting to CD4+ cells of recombinant vesicular stomatitis viruses encoding human immunodeficiency virus envelope proteins. J Virol **71:**5060–5068.
54. **Mebatsion T, Conzelmann KK.** 1996. Specific infection of CD4+ target cells by recombinant rabies virus pseudotypes carrying the HIV-1 envelope spike protein. Proc Natl Acad Sci U S A **93:**11366–11370. http://dx.doi.org/10.1073/pnas.93.21.11366.
55. **Khetawat D, Broder CC.** 2010. A functional henipavirus envelope glycoprotein pseudotyped lentivirus assay system. Virol J **7:**312. http://dx.doi.org/10.1186/1743-422X-7-312.
56. **Tamin A, Harcourt BH, Lo MK, Roth JA, Wolf MC, Lee B, Weingartl H, Audonnet JC, Bellini WJ, Rota PA.** 2009. Development of a neutralization assay for Nipah virus using pseudotype particles. J Virol Methods **160:**1–6. http://dx.doi.org/10.1016/j.jviromet.2009.02.025.
57. **Siler CA, McGettigan JP, Dietzschold B, Herrine SK, Dubuisson J, Pomerantz RJ, Schnell MJ.** 2002. Live and killed rhabdovirus-based vectors as potential hepatitis C vaccines. Virology **292:**24–34. http://dx.doi.org/10.1006/viro.2001.1212.
58. **Johnson JE, Rodgers W, Rose JK.** 1998. A plasma membrane localization signal in the HIV-1 envelope cytoplasmic domain prevents localization at sites of vesicular stomatitis virus budding and incorporation into VSV virions. Virology **251:**244–252. http://dx.doi.org/10.1006/viro.1998.9429.
59. **Rose JK, Bergmann JE.** 1983. Altered cytoplasmic domains affect intracellular transport of the vesicular stomatitis virus glycoprotein. Cell **34:**513–524. http://dx.doi.org/10.1016/0092-8674(83)90384-7.
60. **Foley HD, McGettigan JP, Siler CA, Dietzschold B, Schnell MJ.** 2000. A recombinant rabies virus expressing vesicular stomatitis virus glycoprotein fails to protect against rabies virus infection. Proc Natl Acad Sci U S A **97:**14680–14685. http://dx.doi.org/10.1073/pnas.011510698.
61. **Witting SR, Vallanda P, Gamble AL.** 2013. Characterization of a third generation lentiviral vector pseudotyped with Nipah virus envelope proteins for endothelial cell transduction. Gene Ther **20:**997–1005. http://dx.doi.org/10.1038/gt.2013.23.
62. **Faber M, Faber ML, Li J, Preuss MA, Schnell MJ, Dietzschold B.** 2007. Dominance of a nonpathogenic glycoprotein gene over a pathogenic glycoprotein gene in rabies virus. J Virol **81:**7041–7047. http://dx.doi.org/10.1128/JVI.00357-07.
63. **Schulte S, Sukhova GK, Libby P.** 2008. Genetically programmed biases in Th1 and Th2 immune responses modulate atherogenesis. Am J Pathol **172:**1500–1508. http://dx.doi.org/10.2353/ajpath.2008.070776.